



The Second International Conference on Mining Engineering and Metallurgical  
Technology

# Effect of Slag Composition on Inclusion Control in LF-VD Process for Ultra-low Oxygen Alloyed Structural Steel

Yu TANG

CISDI Group Co., Ltd.

NO.1, Saidi Road, Jinyu Avenue, Yubei District 401122, Chongqing, China

## Abstract

Inclusion control in LF-VD process for ultra-low oxygen alloyed structural steel is investigated. It is found that after Al-deoxidation during tapping process, with slag of high basicity, high  $\text{Al}_2\text{O}_3$  content and low oxidizing property,  $\text{Al}_2\text{O}_3$  inclusions, which are the product of Al-deoxidation could transform to  $\text{MgO-Al}_2\text{O}_3$  spinel, and later on to  $\text{CaO-MgO-Al}_2\text{O}_3$  inclusions of lower melting point, which are inclined to be eliminated by floatation, thus total oxygen content would be lowered. On the other hand, residual inclusions in steel are mostly ultra-fine in size, and could be deformed slightly in hot-working process of steel, enhancing fatigue life of steel.

© 2011 Published by Elsevier Ltd. Open access under [CC BY-NC-ND license](http://creativecommons.org/licenses/by-nc-nd/3.0/).

*Key words:* slag; inclusion; ultra-low oxygen; refining

## 1. Introduction

Alloyed structural steel suffers from recycling and alternative stress in its service life, leading to fatigue destruction, one of the main failing forms. Hard, brittle and un-deformable non-metallic inclusions are usually the origin of fatigue crack. Therefore, this kind of inclusions must be controlled properly in order to enhance fatigue performance of steel. As for Al-killed alloyed structural steel, the majority of inclusions at the beginning of refining are  $\text{Al}_2\text{O}_3$  inclusions of high melting point, un-deformable, with edges and corners, causing clogging of nozzles, as well as ruining fatigue performance of steel.

Previous reports on inclusion control show that during refining process of ultra-low oxygen steel, with the decrease of total oxygen content,  $\text{MgO-Al}_2\text{O}_3$  spinel would appear<sup>[1,2]</sup>, which would be promoted by the increase of  $\text{MgO}$ ,  $\text{Al}_2\text{O}_3$ ,  $\text{CaO/SiO}_2$ ,  $\text{CaO/Al}_2\text{O}_3$  in slag<sup>[3-6]</sup>. However,  $\text{SiO}_2$  in slag would suppress reduction of  $\text{MgO}$ ,  $\text{CaO}$  in slag by  $[\text{Al}]$ s in steel, which is not beneficial for transformation of the product of Al deoxidation. Previous reports on calcium treatment show that calcium treatment would transform inclusions of high melting point to those of lower melting point, protecting nozzles from clogging.

Yu TANG. Tel.: +86-139-8376-0676

E-mail address: [histeven614@163.com](mailto:histeven614@163.com)

However, if calcium treatment is not controlled well,  $\text{CaO-Al}_2\text{O}_3$  of high melting point and  $\text{CaS}$  inclusions would appear, also leading to clogging of nozzles<sup>[9-12]</sup>. In addition, when Si-Ca cored wire is fed into molten steel, it is easy to boil intensively, leading to reoxidation.

Technique of inclusion control by top slag is used for Al-killed steel, aiming to transform  $\text{Al}_2\text{O}_3$  inclusions to  $\text{CaO-MgO-Al}_2\text{O}_3$  inclusions of lower melting point, slightly deformable in hot-working process of steel, achieving ultra-low content of total oxygen and making inclusions' composition enter  $1500^\circ\text{C}$  liquid zone of  $\text{CaO-MgO-Al}_2\text{O}_3$  ternary phase diagram, enhancing fatigue performance of alloyed structural steel.

## 2. Experimental and Results

### 2.1. Experimental

Three furnaces are studied in plant. Production flow is  $\text{LD} \rightarrow \text{LF} \rightarrow \text{VD} \rightarrow \text{calcium treatment} \rightarrow \text{soft bottom-blown by Ar bubbling} \rightarrow \text{continuous casting}$ . Calcium treatment is used in former two furnaces in order to make sure of smooth casting, while the third furnace is exempted from calcium treatment. With Al-deoxidation during tapping and top slag of high basicity, high  $\text{Al}_2\text{O}_3$  content, and low oxidizing property, interaction of slag-steel-inclusion would happen, making inclusions' composition into  $1500^\circ\text{C}$  liquid zone of  $\text{CaO-MgO-Al}_2\text{O}_3$  ternary phase diagram. Steel and slag samples are fetched all through the whole process from beginning of LF to continuous casting. Concrete sampling points are beginning of LF, early stage of LF, middle stage of LF, late stage of LF, end point of LF, after VD, after calcium treatment, after soft bottom-blown by Ar bubbling, 30 and 60 tons of molten steel casted in tundish, 1/2 and 3/4 radius of round billet, abbreviated as LF1, LF2, LF3, LF4, LF5, VD1, VD2, VD3, CC1, CC2, 1/2R, 3/4R in following discussion. Number and size distribution of inclusions are studied by Leica optical microscope. Morphology and composition of inclusions are investigated by SEM-EDS. Chemical composition of steel and slag samples is analyzed at NACIS (National Analysis Center of Iron & Steel).

### 2.2. Results

#### 2.2.1 Achievements of $T[\text{O}]$ control

Table 1 shows average chemical composition of round billets in this experiment. It is shown by table 1 that averaged  $T[\text{O}]$  in billets is 0.0007%, symbolizing high cleanness of final product.

Table 1 Average chemical composition of round billets, %

C	Si	Mn	P	S	Als	Ca	Ti	Cr	T[O]	N
0.60	0.30	0.73	0.015	0.0017	0.029	0.0007	0.0056	0.18	0.0007	0.0034

Fig.1 shows changes of  $T[\text{O}]$  through the whole process. LF1 does not show data of NO.1 furnace because of failed sampling. VD2 only shows data of NO.1 furnace because of failed sampling of NO.2 furnace and exemption of NO.3 furnace from calcium treatment. It is shown by Fig.1 that  $T[\text{O}]$  increases before LF4 or LF5, after that it decreases.  $T[\text{O}]$  of NO.3 furnace at VD3 suddenly rises owing to reoxidation by sampling after breaking hard slag layer, not relevant to experimental process. It can also be seen from Fig.1 that from VD to continuous casting,  $T[\text{O}]$  stabilizes at the range of 0.0006~0.0009%, showing good shielded casting.

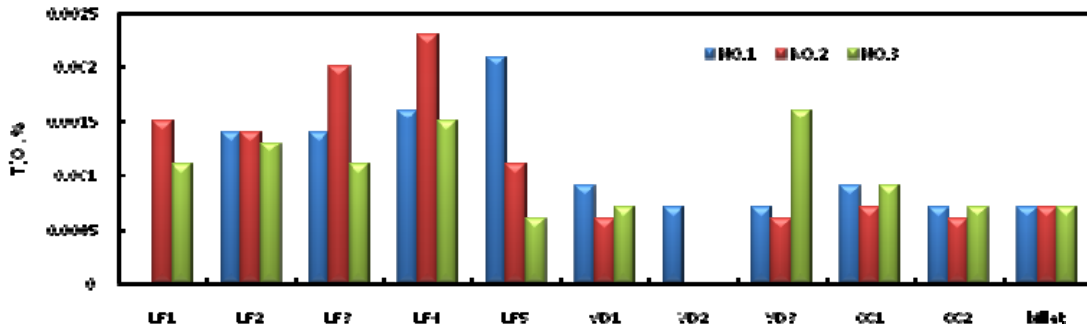


Fig.1 Changes of T[O] through the whole process, %

### 2.2.2 Achievements of inclusion control

Fig.2 shows changes of number of inclusions through the whole process. It is shown by Fig.2 that number of inclusions is inclined to decrease generally, and number of inclusions in round billet is lowered to 10~15/mm<sup>2</sup>. Inclusions in LF-VD process are mainly considered, and calcium treatment is after VD, so composition changes of inclusions do not be discussed respectively between calcium-treated furnace and non-calcium-treated furnace.

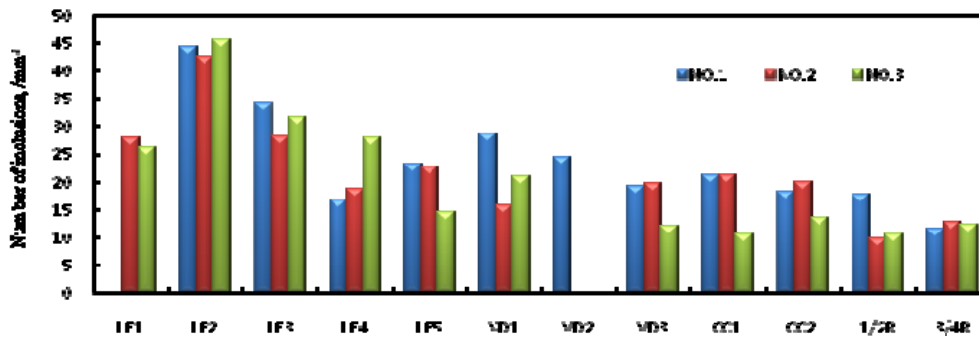
Fig.2 Changes of number of inclusions through the whole process, /mm<sup>2</sup>

Fig.3 shows three kinds of oxide inclusions in refining process. Inclusions transform by sequence of a) → b) → c). Main inclusion at LF1 is Al<sub>2</sub>O<sub>3</sub>, which transforms to MgO-Al<sub>2</sub>O<sub>3</sub> from LF1 to LF4, and some CaO-MgO-Al<sub>2</sub>O<sub>3</sub> inclusions appear at this moment. After that, inclusions transform to CaO-MgO-Al<sub>2</sub>O<sub>3</sub>, and some MgO-Al<sub>2</sub>O<sub>3</sub> inclusions still exist. CaO-MgO-Al<sub>2</sub>O<sub>3</sub> takes up the majority of inclusions after LF process. Because [Ca] in steel would reduce MgO in MgO-Al<sub>2</sub>O<sub>3</sub> inclusion from its outside, morphology of CaO-MgO-Al<sub>2</sub>O<sub>3</sub> complex inclusion is cored structure, whose inside is MgO-Al<sub>2</sub>O<sub>3</sub>, outside is CaO-Al<sub>2</sub>O<sub>3</sub> of lower melting point, reducing harm of MgO-Al<sub>2</sub>O<sub>3</sub> spinel to steel performance.

Fig.4 shows line scan and element mapping of CaO-MgO-Al<sub>2</sub>O<sub>3</sub> inclusion. It can be seen that MgO-Al<sub>2</sub>O<sub>3</sub> spinel exists inside CaO-MgO-Al<sub>2</sub>O<sub>3</sub> inclusion, cored by CaO-Al<sub>2</sub>O<sub>3</sub>.

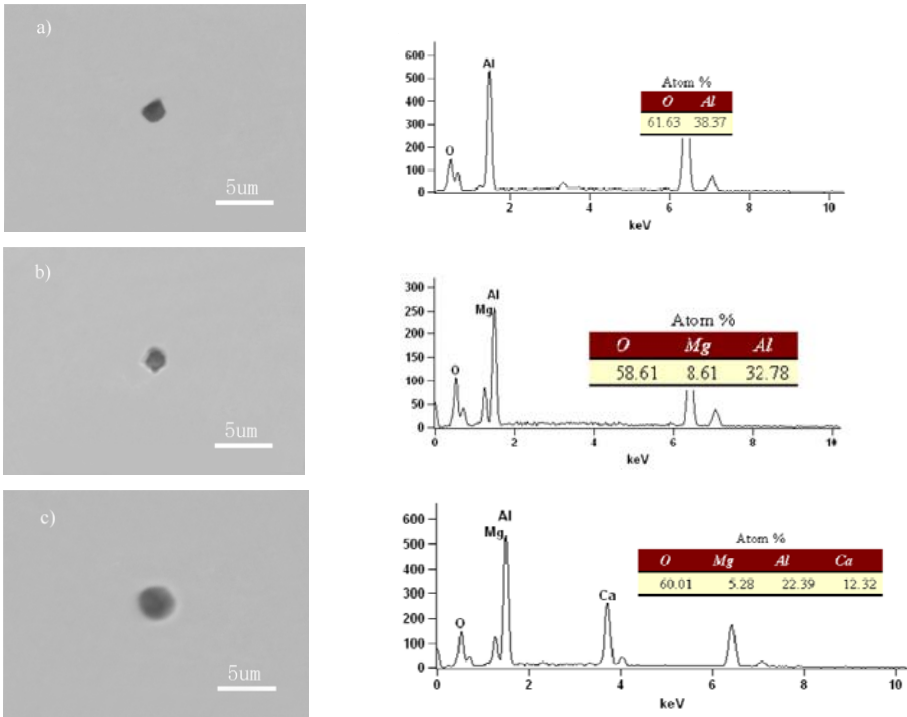


Fig.3 Three kinds of oxide inclusions in refining process a)  $\text{Al}_2\text{O}_3$ ; b)  $\text{MgO-Al}_2\text{O}_3$ ; c)  $\text{CaO-MgO-Al}_2\text{O}_3$

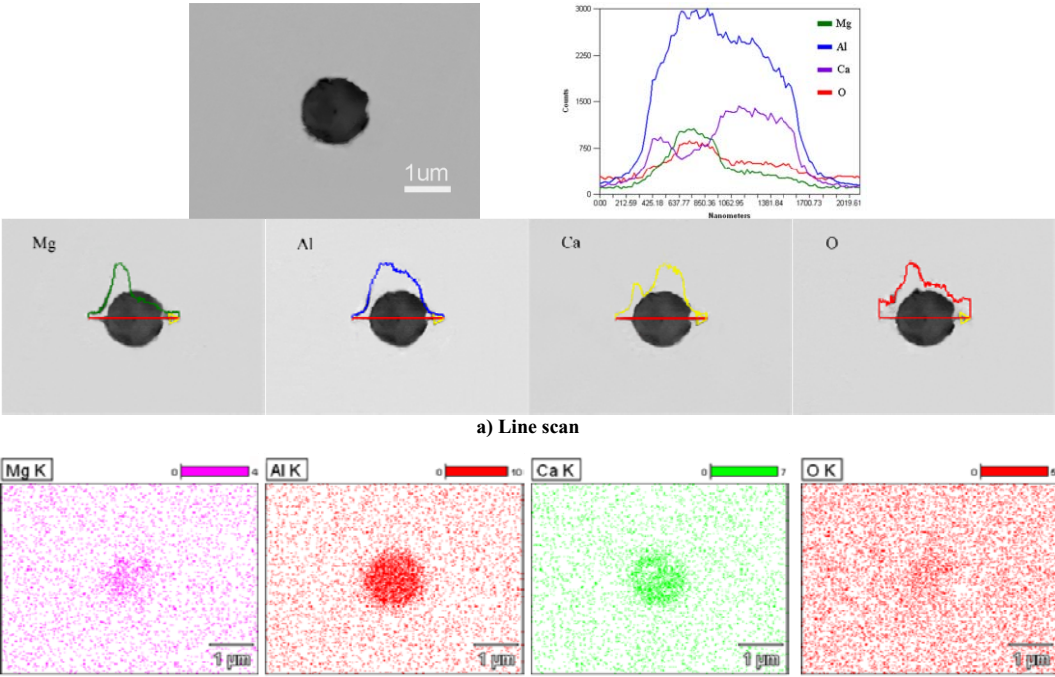


Fig.4 Line scan and mapping of  $\text{CaO-MgO-Al}_2\text{O}_3$  inclusion

### 3. Discussion

Inclusion control by top slag is realized by slag-steel interaction and steel-inclusion interaction. Following discussions are made according to this mechanism.

#### 3.1. Slag-steel interaction

During LF process, [Mg], [Ca] in steel increases gradually, owing to slag-steel reactions shown as (1), (2), letting (MgO), (CaO) in slag be reduced by [Al]s in steel. The other source of MgO is furnace lining.

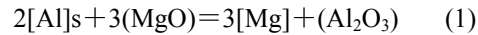


Fig.5 shows changes of (CaO), (MgO), ( $\text{Al}_2\text{O}_3$ ) in slag. It is shown by Fig.5 that (CaO) stabilizes at about 50% in LF process, then declines to 42% after VD. This is because refining slag is added several times during LF process, resuming (CaO) in slag consumed on reduction by [Al]s in steel. (MgO) keeps general rising trend in LF-VD process from 5.7~10%. (MgO) is supposed to decline if the reaction shown as (1) is only considered, but actual data rises because MgO in furnace lining enters slag, and added refining slag contains MgO. ( $\text{Al}_2\text{O}_3$ ) shows slight rising trend in LF process, then rises suddenly to 39% after VD as a result of three factors: (i) Al particles are added into slag for diffusion deoxidation; (ii)  $\text{Al}_2\text{O}_3$ , product of the reactions shown as (1), (2) enters slag; (iii) inclusions are absorbed by slag.

Fig.6 shows changes of [Ca], [Mg], [Al]s in steel. If the reactions shown as (1), (2) are only considered, [Al]s is supposed to decline. However, it is shown by Fig.6 that [Al]s rises to 0.084% at LF3, then declines to 0.018% at VD1, because Al particles are added into slag for diffusion oxidation in early stage of LF process, leading to the increase of [Al]s in steel, much more than the amount of [Al]s oxidized by (MgO), (CaO) in slag. [Mg], [Ca] in steel rises to 0.0007% and 0.0012% respectively at LF4, because the product of reduction of (MgO), (CaO) by [Al]s enters molten steel. After LF4, [Mg], [Ca] in steel declines to 0.0005% and 0.0008% respectively at VD1 because of vaporization and reaction with inclusions.

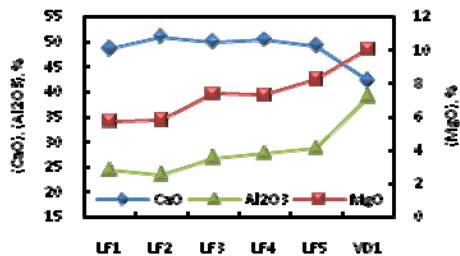


Fig.5 Changes of (CaO), (MgO), ( $\text{Al}_2\text{O}_3$ ) in slag

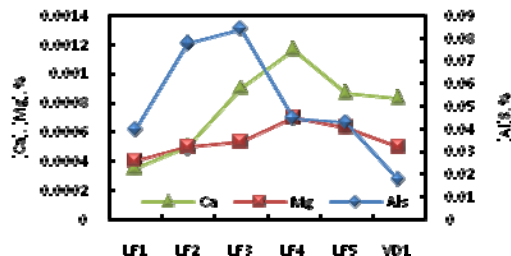


Fig.6 Changes of [Ca], [Mg], [Al]s in steel

Fig. 7 shows effect of slag basicity on [Mg], [Ca] in steel. It is shown by Fig.7 that [Mg], [Ca] in steel increases as slag basicity increases. When R is about 10, [Mg], [Ca] in steel is 0.0006% and 0.0011%

respectively. It can be deduced that high basicity slag would promote the reactions shown as (1), (2), however which are suppressed by ( $\text{SiO}_2$ ) in slag, keeping good accordance to references<sup>[7, 8]</sup>.

Fig.8 shows effect of ( $\text{FeO}+\text{MnO}$ ) in slag on  $[\text{Mg}]$ ,  $[\text{Ca}]$  in steel. It is shown by Fig.8 that  $[\text{Mg}]$ ,  $[\text{Ca}]$  in steel increases as ( $\text{FeO}+\text{MnO}$ ) in slag decreases. When ( $\text{FeO}+\text{MnO}$ ) in slag is 0.9%,  $[\text{Mg}]$ ,  $[\text{Ca}]$  in steel is 0.0007% and 0.0011% respectively. It can be deduced that slag with low oxidizing property promotes the reactions shown as (1), (2).

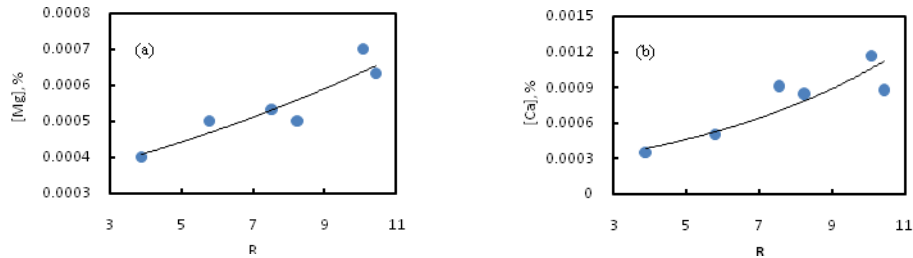


Fig.7 Effect of slag basicity on (a)  $[\text{Mg}]$ , (b)  $[\text{Ca}]$  in steel

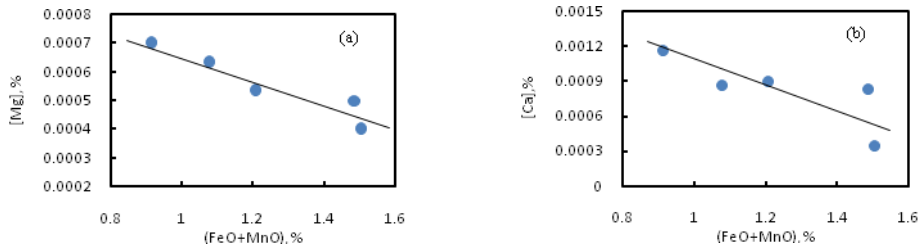
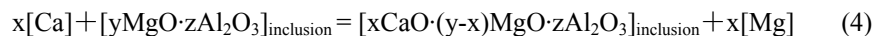


Fig.8 Effect of ( $\text{FeO}+\text{MnO}$ ) in slag on (a)  $[\text{Mg}]$ , (b)  $[\text{Ca}]$  in steel

### 3.2. Steel-inclusion interaction

With increase of  $[\text{Mg}]$ ,  $[\text{Ca}]$  in steel, steel-inclusion interaction would happen, shown as (3), (4), transforming  $\text{Al}_2\text{O}_3$  gradually to  $\text{MgO}-\text{Al}_2\text{O}_3$ , then to  $\text{CaO}-\text{MgO}-\text{Al}_2\text{O}_3$  complex inclusions with lower melting point.



With high basicity slag, Mg reduced from  $\text{MgO}$  by  $[\text{Al}]$ s enters molten steel. So it is inevitable for the formation of  $\text{MgO}-\text{Al}_2\text{O}_3$  spinel, which was also proven in references<sup>[1, 2]</sup>. Nevertheless, if the reaction shown as (4) performs fully, there would be an adequately thick layer of  $\text{CaO}-\text{Al}_2\text{O}_3$  of lower melting point outside  $\text{MgO}-\text{Al}_2\text{O}_3$ , whose harm would be reduced.

Fig.9 shows changes of average composition proportion in inclusions. It is shown by Fig.9 that with the progress of refining, proportion of  $\text{Al}_2\text{O}_3$  in inclusions decreases gradually from 97.8% at LF1 to 62.7% at LF4, then increases slightly to 66.9% at VD1. Proportion of MgO in inclusions increases from 1.6% at LF1 to 13.5% at LF4, then decreases to 7.8% at VD1. Proportion of CaO in inclusions increases from 0.6% at LF1 to 25.2% at VD1, a little bit later than the increase of the proportion of MgO, owing to the sequent progress of reactions shown as (3), (4). Before LF4,  $\text{Al}_2\text{O}_3$  inclusion transforms to  $\text{MgO-Al}_2\text{O}_3$ , raising the proportion of MgO in inclusions. The transformation of  $\text{MgO-Al}_2\text{O}_3$  to  $\text{CaO-MgO-Al}_2\text{O}_3$  happens a little bit later than the transformation of  $\text{Al}_2\text{O}_3$  to  $\text{MgO-Al}_2\text{O}_3$ , but it plays the major role after LF4, raising the proportion of CaO in inclusions, and reducing the proportion of MgO in inclusions because of the reduction of MgO in inclusions by  $[\text{Ca}]$  in steel.

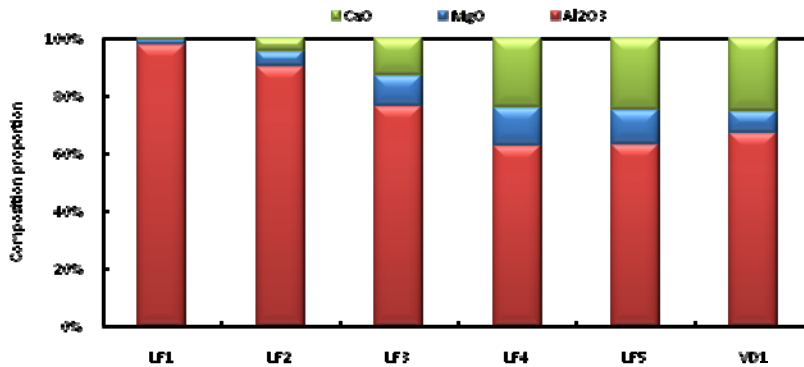


Fig.9 Changes of average composition proportion in inclusions

Fig.10 shows effect of  $[\text{Mg}]$  in steel on MgO in inclusions and Fig.11 shows effect of  $[\text{Ca}]$  in steel on CaO in inclusions. It is shown by Fig.10 that MgO in inclusions increases as  $[\text{Mg}]$  in steel increases, and by Fig.11 that CaO in inclusions increases as  $[\text{Ca}]$  in steel increases. When  $[\text{Mg}]$  content in steel is 0.0007%, MgO content in inclusions is 10.5%. When  $[\text{Ca}]$  content in steel is 0.0009~0.0012%, CaO content in inclusions is 16.7~21.4%. It can be deduced that  $[\text{Mg}]$ ,  $[\text{Ca}]$  in steel respectively promotes the reactions shown as (3), (4).

Extent of reactions shown as (3), (4) can be described by  $\text{MgO}/\text{Al}_2\text{O}_3$  and  $\text{CaO}/\text{MgO}$  respectively. Fig.12 shows effect of  $[\text{Mg}]$  in steel on  $\text{MgO}/\text{Al}_2\text{O}_3$  in inclusions. Fig.13 shows effect of  $[\text{Ca}]$  in steel on  $\text{CaO}/\text{MgO}$  in inclusions. It is shown by Fig.12 that  $\text{MgO}/\text{Al}_2\text{O}_3$  in inclusions increases as  $[\text{Mg}]$  in steel increases, and by Fig.13 that  $\text{CaO}/\text{MgO}$  in inclusions increases as  $[\text{Ca}]$  in steel increases. When  $[\text{Mg}]$  content in steel is 0.0007%,  $\text{MgO}/\text{Al}_2\text{O}_3$  in inclusions is 0.22. When  $[\text{Ca}]$  content in steel is 0.0009~0.0012%,  $\text{CaO}/\text{MgO}$  in inclusions is 1.76~2.

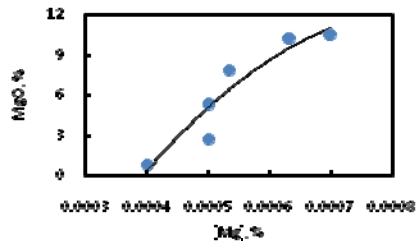


Fig.10 Effect of [Mg] in steel on MgO in inclusions

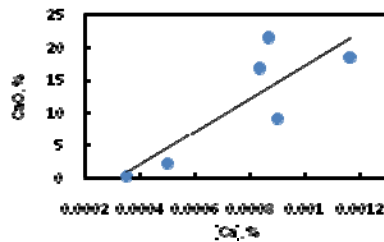


Fig.11 Effect of [Ca] in steel on CaO in inclusions

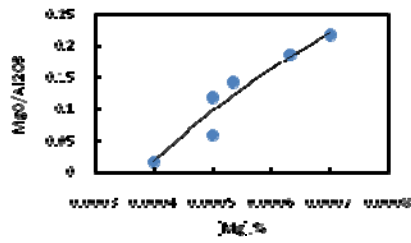
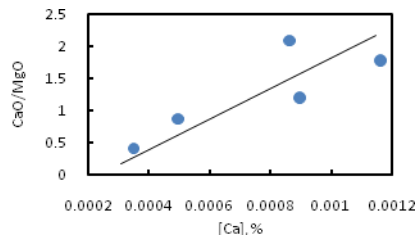
Fig.12 Effect of [Mg] in steel on MgO/Al<sub>2</sub>O<sub>3</sub> in inclusions

Fig.13 Effect of [Ca] in steel on CaO/MgO in inclusions

Fig.14 shows inclusion transformation route in LF-VD process by projecting average composition of all inclusions at every sampling point in LF-VD process (LF1~VD1) to ternary phase diagram of CaO-MgO-Al<sub>2</sub>O<sub>3</sub>. The blue shaded area symbolizes 1500°C liquid zone, which is the target zone for inclusion control. It is shown by Fig.14 that the majority of inclusions are Al<sub>2</sub>O<sub>3</sub> at the beginning of LF. With the progress of refining, spots of inclusions' composition close to 1500°C liquid zone gradually, and begin to enter this zone since late stage of LF, although not completely. Inclusion transformation is a persistent and time-consuming process of slag-steel-inclusion bounding to equilibrium. However, time of LF-VD process is not adequate for complete inclusion transformation. But fortunately, there is plenty of time for inclusions to continue to transform from the end point of VD to solidification of molten steel. In the end, most inclusions' composition would enter 1500°C liquid zone.

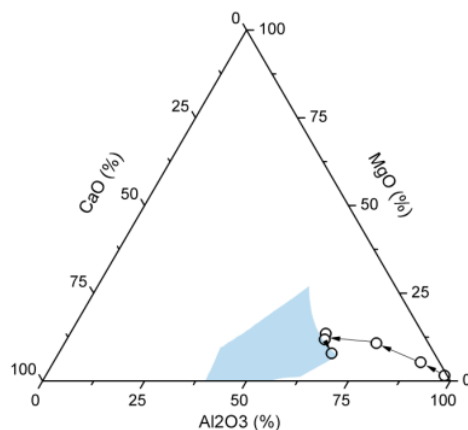


Fig.14 Inclusion transformation routine in LF-VD process



#### 4. Conclusions

Under the condition of Al deoxidation and slag of high basicity, high  $\text{Al}_2\text{O}_3$  content and low oxidizing property, effect of slag composition on inclusion control in LF-VD process for ultra-low oxygen alloyed structural steel is investigated. Conclusions are drawn as below.

- 1) On one hand, low content of soluble oxygen is achieved by Al-deoxidation. On the other hand, most liquid inclusions would be eliminated by floatation. Both would lower the content of T[O] to 0.0007% in round billets, achieving high cleanness of steel;
- 2) Slag composition is controlled well in LF process, which would be beneficial to get proper composition of molten steel to promote the transformation of  $\text{Al}_2\text{O}_3 \rightarrow \text{MgO-Al}_2\text{O}_3 \rightarrow \text{CaO-MgO-Al}_2\text{O}_3$ . Most inclusions' composition would begin to enter 1500°C liquid zone from late stage of LF process, owing to proper composition of molten steel, which is beneficial for inclusions to continue to transform and to be eliminated by floatation until solidification of molten steel;
- 3) Number of inclusions decreases apparently owing to agglomeration and floatation. Inevitably residual inclusions in steel are spherical or spherical-alike inclusions with ultra-fine size, lower melting point and slight deformability in hot-working process of steel.

#### References

- [1] SUIITO Hideaki, et al. Thermodynamics on Control of Inclusions Composition in Ultra-clean Steels. ISIJ International, 1996, 36 (5): 528-536.
- [2] NISHIMORI H, et al. Bull. Jpn. Inst. Met., 1993, 1: 441.
- [3] HOJO Masatake, et al. Oxide Inclusion Control in Ladle and Tundish for Producing Clean Stainless Steel. ISIJ International, 1996, 36(Supplement): S128-S131.
- [4] KIM Jong wan, et al. Formation Mechanism of Ca-Si-Al-Mg-Ti-O Inclusions In Type 304 Stainless Steel. ISIJ International, 1996, 36(Supplement): S140-S143.
- [5] JIANG Min, et al. Formation of  $\text{MgO-Al}_2\text{O}_3$  inclusions in high strength alloyed structural steel refined by  $\text{CaO-SiO}_2\text{-Al}_2\text{O}_3\text{-MgO}$  slag. ISIJ International, 2008, 48 (7): 885-890.
- [6] OKUYAMA Goro, et al. Effect of Slag Composition on the Kinetics of Formation of  $\text{Al}_2\text{O}_3\text{-MgO}$  Inclusions in Aluminum Killed Ferritic Stainless Steel. ISIJ International, 2000 40 (2): 121-128.
- [7] TODOROK Hidekazu, et al. Effect of Silica in Slag on Inclusion Compositions in 304 Stainless Steel Deoxidized with Aluminum. ISIJ International, 2004, 44 (8): 1350-1357.
- [8] SUN Haiping, et al. Oxidation Rate of Aluminum in Molten Iron by  $\text{CaO-SiO}_2\text{-Al}_2\text{O}_3\text{-FeO-MnO}$  Slag. ISIJ International, 1996, 36 (Supplement): S34-S37.
- [9] HOLAPPA L E K, et al. Inclusion Control in High-Performance Steels. Journal of Materials Processing Technology, 1995, 53:177-186.
- [10] HIGUCHI Yoshihiko, et al. Inclusion Modification by Calcium Treatment. ISIJ International, 1996, 36 (Supplement): S151-S154.
- [11] KUSANO Yoshiaki, et al. Calcium Treatment Technologies for Special Steel Bars and Wire Rods. ISIJ International, 1996, 36 (Supplement): S77-S80.
- [12] YE Guozhu, et al. Thermodynamics and Kinetics of the Modification of  $\text{Al}_2\text{O}_3$  Inclusions. ISIJ International, 1996, 36 (Supplement): S105-S108.